5.6 NUMERICAL SIMULATIONS OF AIR FLOWS IN AND AROUND A CITY IN A COASTAL REGION

Tetsuji Yamada*
Yamada Science & Art Corporation, Santa Fe, New Mexico

1. INTRODUCTION

Urbanization has drastically increased at an alarming rate. In the 1800's, only three percent of the world's population lived in urban areas. By the 1950's, thirty percent were urbanized and in 2000 about forty seven percent lived in urban areas (UN,1999). The number of mega-cities (population of 10 million or more people) dramatically increased from four in 1975 to eighteen in 2000. The United Nations estimates there will be around twenty-two mega-cities by 2015 (UN, 2003).

With this ever-increasing growth came numerous problems such as air pollution associated with emissions from automobiles and plants, and temperature increases associated with human activities to name a few. Both issues are considered to be the major contributors to the global warming.

Urban areas are known to be warmer than the surrounding rural areas (so called "urban heat island"). Bare soils and vegetated surfaces are replaced by concrete structures and pavements which absorb and store more heat from the sun than the original surfaces. The heat energy stored in the pavements and concrete structures heat air during the night time. Urban heat island effect is further enhanced by exhaust heat associated with human activities such as air conditioning and manufacturing.

The urban heat island coupled with adverse weather conditions creates serious health problems. Heat waves are blocked by high rises and stay in urban areas causing heat strokes and discomforts to the people living in the urban areas.

Recently, there have been some efforts in combining the CFD and atmospheric models capabilities to address effects on air flows from a building to terrain scales. This is what is required to simulate air flows over the urban areas in complex terrain and/or coastal areas. This paper discusses how an atmospheric model HOTMAC was improved to simulate air flows around buildings under the influence of mesoscale wind variations.

* *Corresponding author address*: Tetsuji Yamada, Yamada Science & Art Corporation, 13 Heiwa, Santa Fe, NM 87506; e-mail: ysausa@ysasoft.com

2. MODELS

The governing equations for mean wind, temperature, mixing ratio of water vapor, and turbulence are similar to those used by Yamada and Bunker (1988). Turbulence equations were based on the Level 2.5 Mellor-Yamada second-moment turbulence-closure model (1974, 1982). Five primitive equations were solved for ensemble averaged variables: three wind components, potential temperature, and mixing ratio of water vapor. In addition, two primitive equations were solved for turbulence: one for turbulence kinetic energy and the other for a turbulence length scale (Yamada, 1983).

The hydrostatic equilibrium is a good approximation in the atmosphere. On the other hand, air flows around buildings are not in the hydrostatic equilibrium. Pressure variations are generated by changes in wind speeds, and the resulted pressure gradients subsequently affect wind distributions. We adopted the HSMAC (Highly Simplified Marker and Cell) method (Hirt and Cox, 1972) for pressure computation because the method is simple yet efficient. The method is equivalent to solving a Poisson equation, which is commonly used in non-hydrostatic atmospheric models.

Boundary conditions for the ensemble and turbulence variables are discussed in detail in Yamada and Bunker (1988). The temperature in the soil layer is obtained by numerically integrating a heat conduction equation. Appropriate boundary conditions for the soil temperature equation are the heat energy balance at the ground and specification of the soil temperature at a certain distance below the surface, where temperature is constant during the integration period. The surface heat energy balance is composed of solar radiation, long-wave radiation, sensitive heat, latent heat, and soil heat fluxes.

Lateral boundary values for all predicted variables are obtained by integrating the corresponding governing equations, except that variations in the horizontal directions are all neglected. The upper level boundary values are specified and these values are incorporated into the governing equations through a four-dimensional data assimilation or a “nudging” method (Kao and Yamada, 1988).

3. SIMULATIONS

Detailed observations are required for model verifications. However, atmospheric observations are expensive and time consuming, thus limited in numbers. For this reason, wind tunnel measurements are often used for verification of model results. Wind tunnel measurements played significant roles for understanding physics of phenomena and providing data for determining parameters in model parameterizations.

Air flows in wind tunnel measurements need to be similar to the air flows in the real atmosphere. Various similarity parameters such as Reynolds number and Froude number must be equal to each other in the wind tunnel and real atmosphere. It is impossible to satisfy all requirements for similarity, thus similarity is only partially satisfied.

HOTMAC was improved so that wind tunnel data are simulated without scaling, thus the similarity requirements are exactly satisfied. Horizontal grid spacing of HOTMAC was reduced to 2 cm to resolve air flows around blocks placed in a wind tunnel. Dimensions of each block were 15 cm (H) x 16 cm (W) x 16 cm (D).

Figure 1 shows the modeled air flows in the vertical cross section along the centerline of the wind tunnel. Wind direction is from left to right. Separation of air flows occurred at the leading edges and recirculation was seen at the roofs of the blocks in the first row. Recirculation is evident in the cavity between the first and second blocks. Flow reattachment was approximately 1.3 times the height of the block (15 cm), which is in good agreement with wind tunnel measurements (Brown et al., 2001).

The modeled turbulence kinetic energy (t.k.e.) and turbulence length scale (t.l.s) are shown in Figs. 2a and 2b, respectively. Large t.k.e. values are seen over the first block and between the first and second block. The t.k.e. over the third block was much smaller than the counterpart over the first and second blocks. Another maximum occurred downstream the last block where wind shear was large suggesting the large t.k.e. production.

The modeled t.l.s.(Fig. 2b) shows large values over the first and second blocks which is similar to the t.k.e. distribution. Two prognostic equations were solved for turbulence: one is for q^2 (twice the t.k.e.) and the other is for $q^2 l$. The length scale, l, was obtained by dividing $q^2 l$ by q^2.

Figure 3 shows measured t.k.e. for 2-D and 3-D blocks in a wind tunnel (Brown et al., 2001). The measured t.k.e. for 2-D blocks was much larger than the counterparts for the 3-D blocks. Acceleration of air flows over the 2-D blocks was much larger than the acceleration over the 3-D blocks resulted in larger production of t.k.e.

Most wind tunnel measurements were conducted under the conditions where boundary conditions did not change with time (steady state) and no heating and cooling effects were considered. In the real atmosphere, however, solar heating and radiation cooling play important roles in generating local circulations such as sea- and land-breezes, and mountain- and valley winds.

We simulated diurnal variations of air flows around a cluster of buildings, which were bound by the ocean and hills. Large cities are often located in a coastal area or near complex terrain. Prediction of transport and diffusion of air pollutants and toxic materials is a considerable interest to the health of the people living in urban areas.

Two inner domains were nested in a large domain (Fig. 4). The first domain was 6560 m x 8960 m with horizontal grid spacing of 160 m. The second domain was 1280 m x 1440 m with horizontal grid spacing of 40 m and the third domain was 360 m x 400 m with horizontal grid spacing of 10 m.

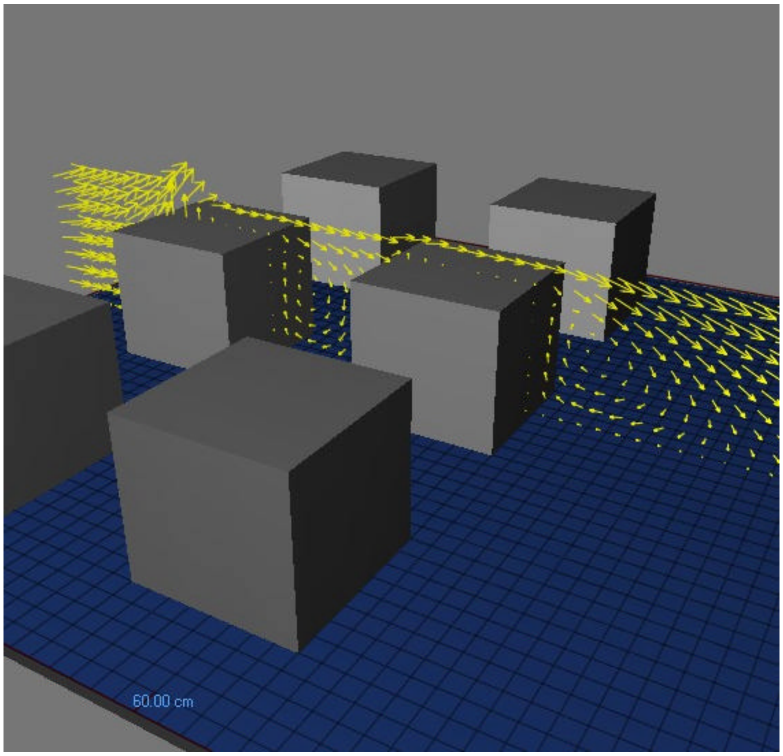

Figure 1: The modeled air flows in the vertical cross section along the centerline of a wind tunnel. The dimensions of each block are 15 cm (H) x 16 cm (W) x 16 cm (D). Horizontal grid spacing of HOTMAC was 2 cm and the vertical grid spacing was 2 cm for the first 20 cm above the wind tunnel floor and increased gradually in the upper layers.

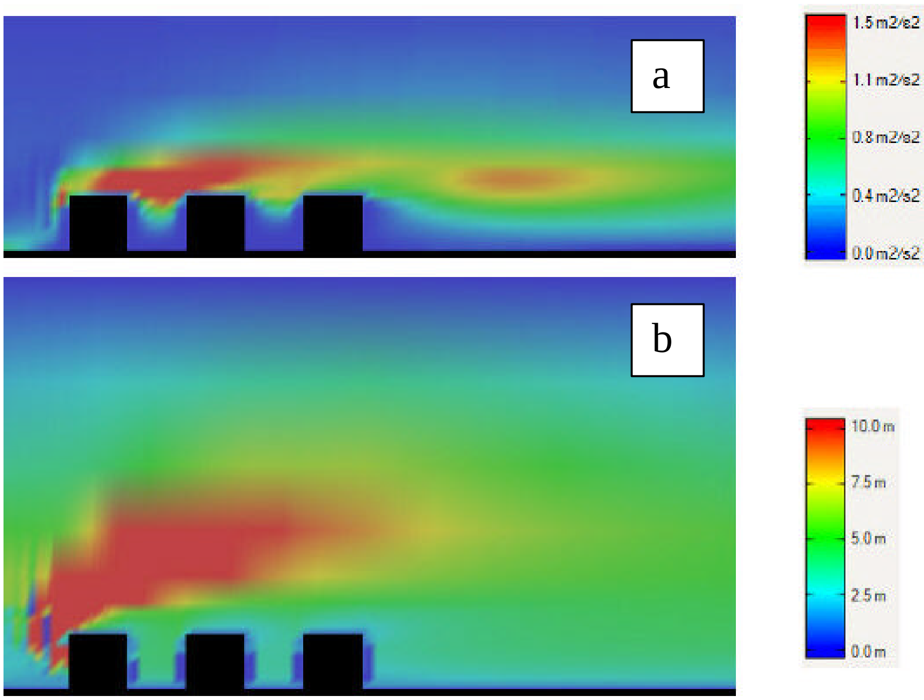

Figure 2: a) The modeled turbulence kinetic energy (t.k.e.) and b) turbulence length scale (t.l.s.) in the vertical section along the centerline.

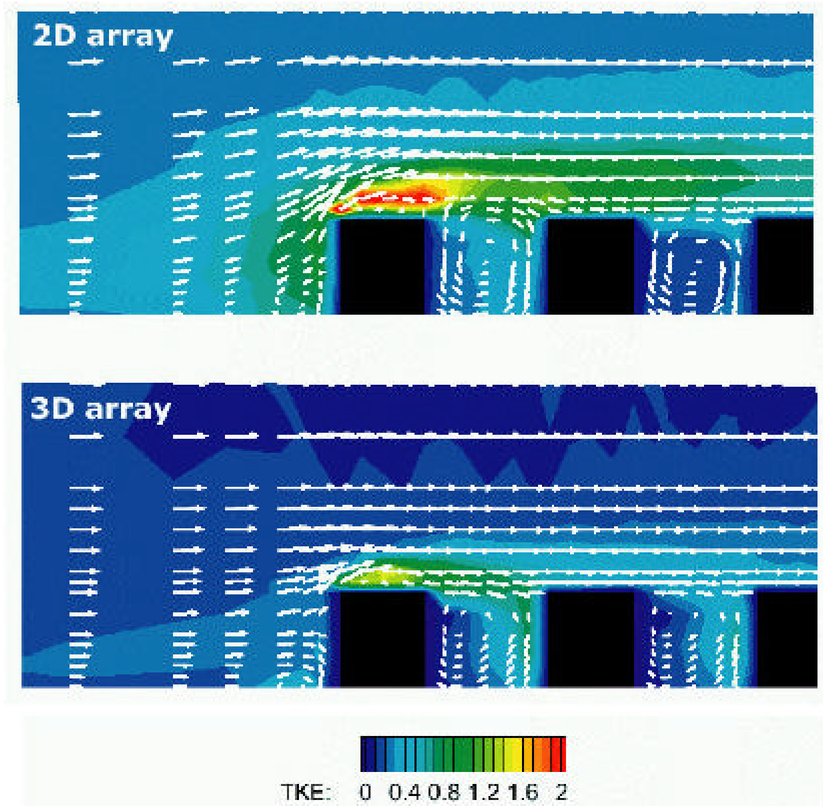

Figure 3: The measured turbulence kinetic energy for 2-D and 3-D blocks in a wind tunnel (Brown et al., 2001)

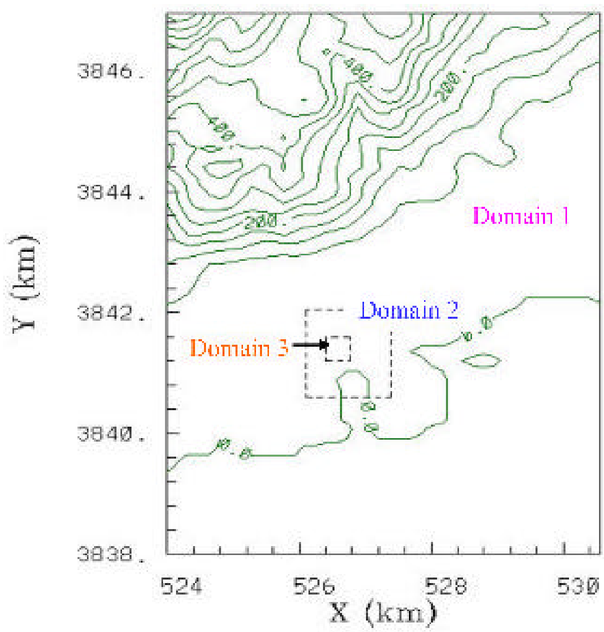

Figure 4: Computational domains: Domain 1 is the outer domain. Solid contour lines indicate ground elevations. Numerical numbers are altitudes in meters. Dashed lines indicate boundaries of nested domains: Domain 2 and Domain 3.

Domain 1 includes topographic features such as the ocean, coastal area, plains, and hills. Domain 2 is a transition area between Domain 1 and Domain 3. Buildings were located in Domain 3.

There were significant interactions between air flows generated by topographic variations and a cluster of buildings. The winds were blocked and the sea breeze fronts were retarded by buildings. Winds were calm in the area surrounded by buildings. Winds diverged in the upstream side and converged in the downstream side of the building cluster (Fig. 5a).

The modeled surface temperatures in the urban area were several degrees higher than those in the surrounding non-building areas. In the present simulation, temperature increasing was caused mainly by the reduction of wind speeds by building blocking. As seen from Fig. 5, higher temperatures (red areas in Fig. 5b) are correlated well with the low wind speeds (Fig. 5a).

Atmospheric turbulence is small where wind speed is small. Sensible heat flux becomes small since it is proportional to turbulence intensity. Decreased sensible heat flux increases the heat flux into the ground in the heat energy balance equation at the ground, resulting in higher ground temperature.

Figure 6 shows the modeled wind speed distributions at 2 m above the ground at 9:10 am in Domain 2. Winds diverged in the upstream side of the building clusters and converged in the downstream side. Winds were accelerated around both sides of the high rises and winds were calm in the area surrounded by buildings. Winds were relatively high over the water and in the coastal areas due to acceleration of winds by sea breezes.

Figure 7 shows the modeled turbulence kinetic energy (t.k.e.) at 4 m above the ground at 9:10 am in Domain 2. The t.k.e. was large around the building clusters where wind speeds were large (Fig. 6). The t.k.e. was considerably smaller over the water than over the land.

Figure 8 shows the modeled temperature distributions in a vertical cross section through high rises at 9:10 am in Domain 2. Roof temperatures were determined from the heat energy balance equation and a heat conduction equation at the roof in a fashion similar to the ground temperature computation. Air temperatures were higher over the high rises, resulting in a heat dorm as shown in Fig. 8.

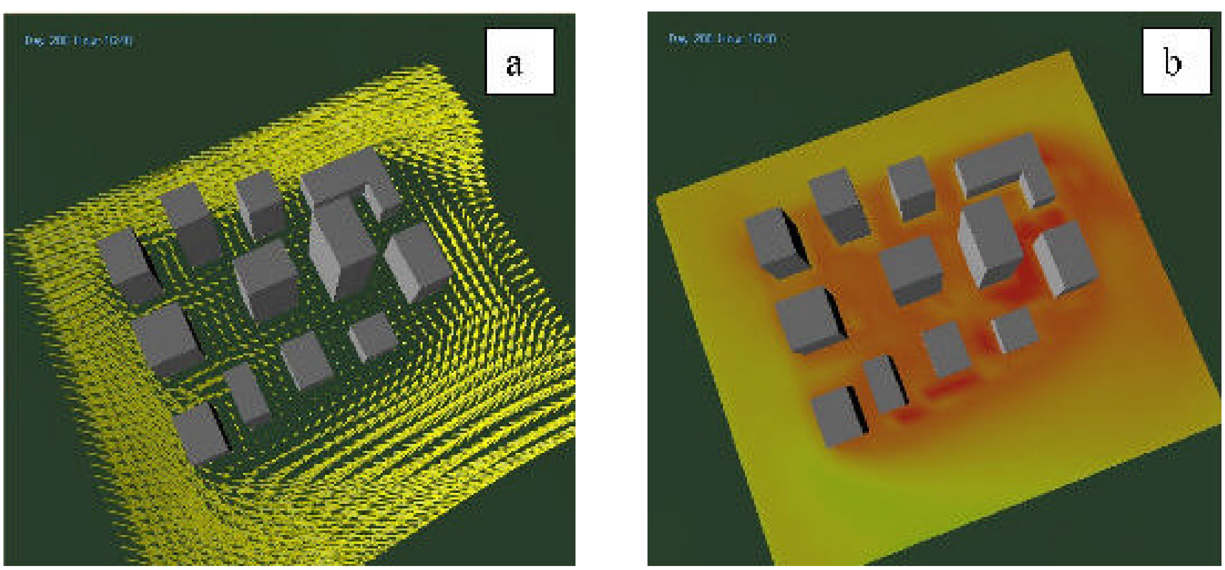

Figure 5: a) The modeled wind distribution at 2 m above the ground and b) the surface temperature distribution in Domain 3 at 16:40 local time.

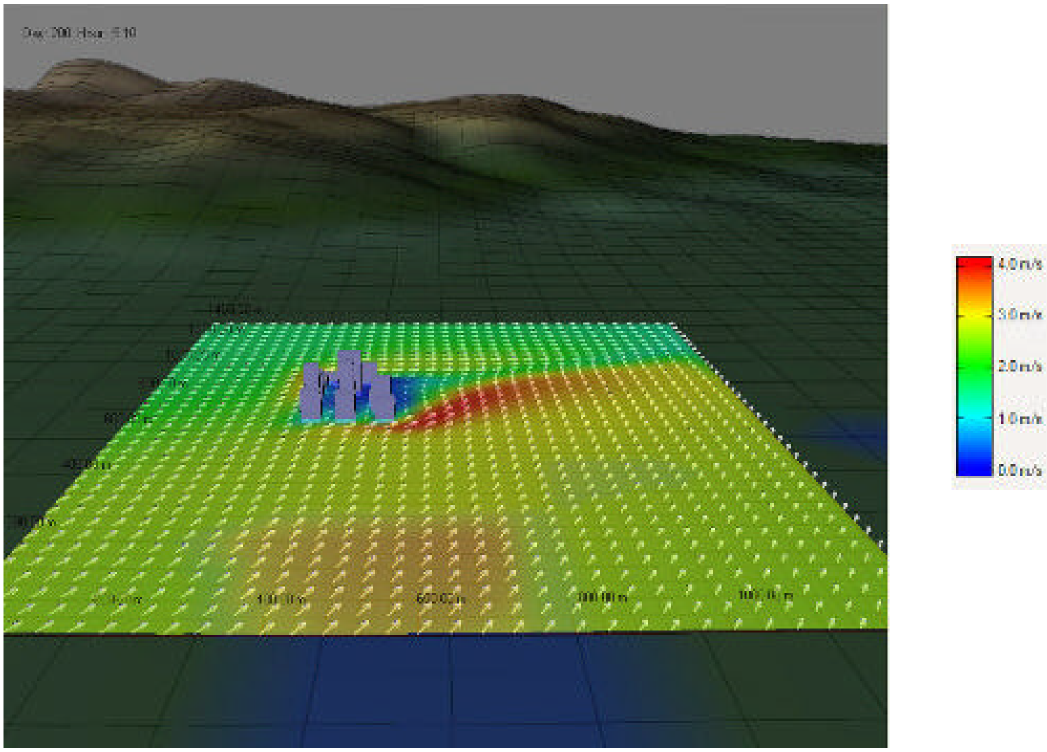

Figure 6: The modeled wind speed distributions at 2m above the ground at 9:10 am in the Domain 2.

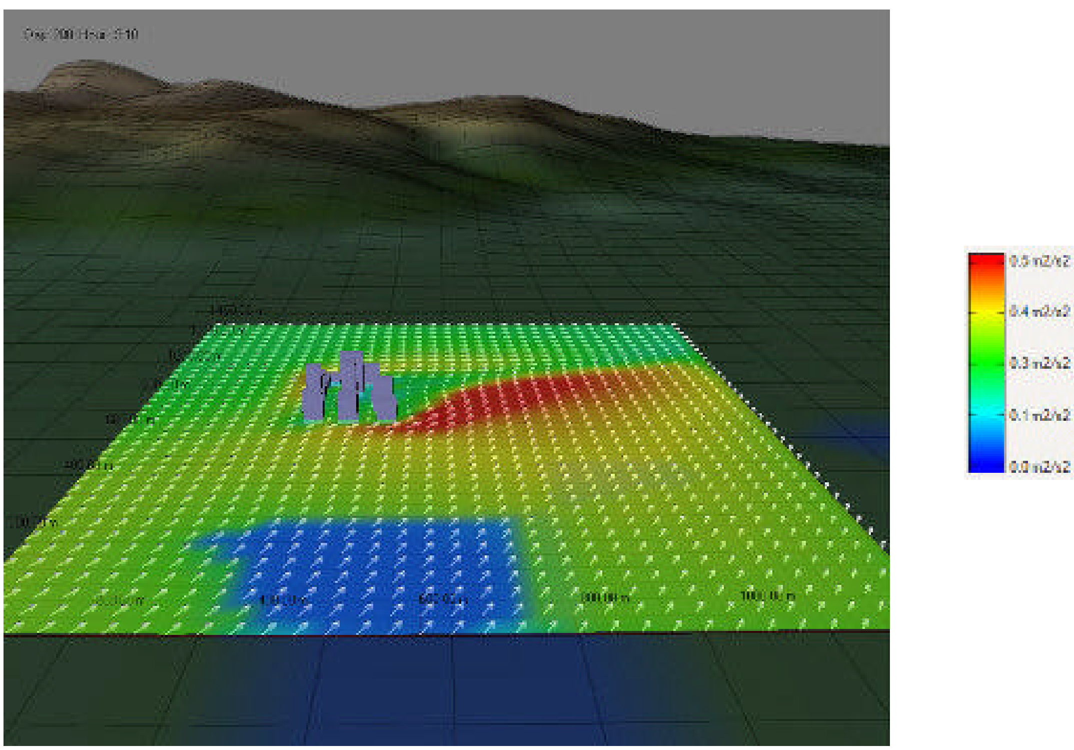

Figure 7: The modeled turbulence kinetic energy (t.k.e.) at 4 m above the ground at 9:10 am in Domain 2.

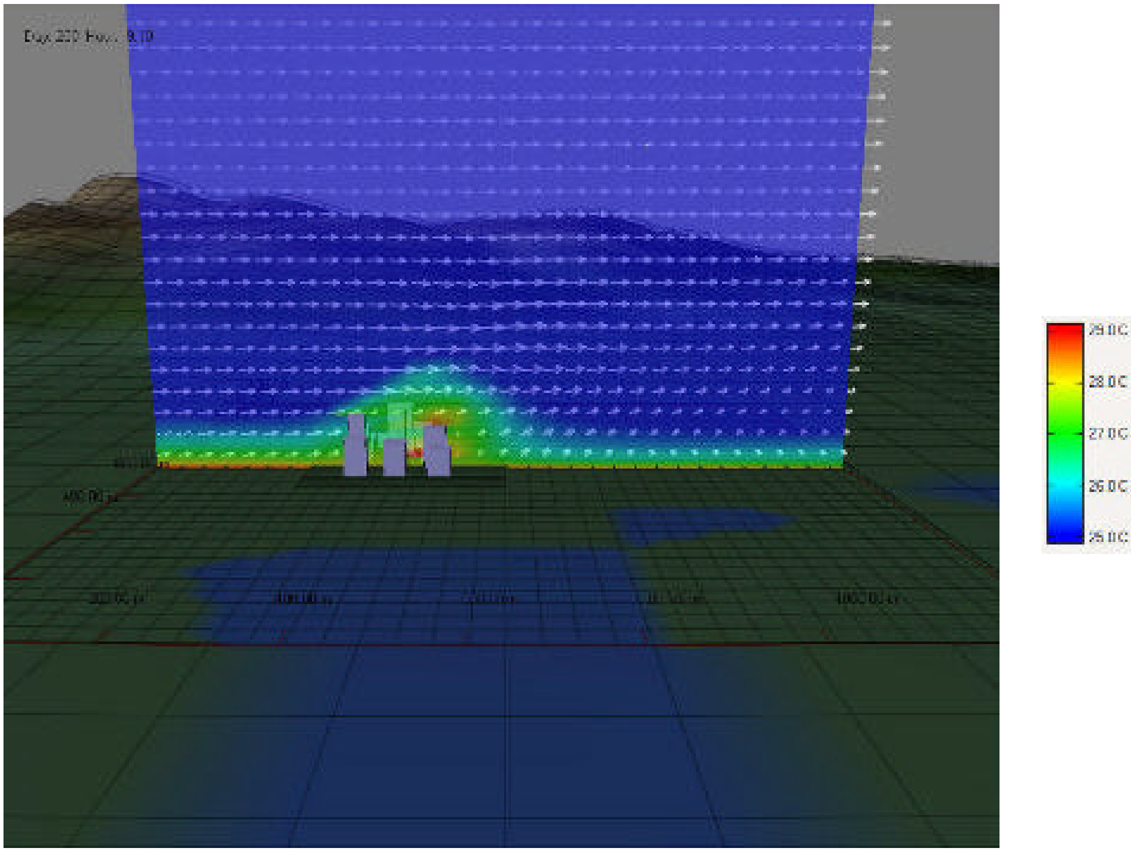

Figure 8: The modeled temperature distributions in a vertical cross section through high rises at 9:10 am in Domain 2.

4. SUMMARY

A three-dimensional atmospheric prediction model, HOTMAC, was improved so that airflows not only in complex terrain, but also around buildings and wind tunnel data were simulated. We adopted HSMAC method for the non-hydrostatic pressure computation because it is simple yet efficient. The method is equivalent to solving a Poisson equation, which is commonly used in non-hydrostatic atmospheric models.

We simulated diurnal variations of air flows around a cluster of buildings, which were bound by the ocean and hills. Large cities are often located in a coastal area or near complex terrain. Prediction of transport and diffusion of air pollutants and toxic materials is of considerable interest to the health of the people living in urban areas.

We deployed nested grids: Domain 1 was 6560 m x 8960 m with horizontal grid spacing of 160 m. Domain2 was 1280 m x 1440 m with 40 m grid spacing and nested in Domain 1. Domain 3 was 360 m x 400 m with 10 m grid spacing and nested in Domain 2.

There were significant interactions between air flows generated by topographic variations and a cluster of buildings. Sea breeze fronts were retarded by buildings. Winds were calm in the courtyards. Winds diverged in the upstream side and converged in the downstream side of the building cluster.

Wind speeds and wind directions around buildings changed as the winds in the outer domains encountered diurnal variations. Domain 3 alone could not reproduce diurnal variations of winds because it didn't include topographic features responsible for local circulations such as sea/land breezes and mountain/valley flows.

On the other hand, Domain 1 alone could not depict the effects of buildings because the horizontal grid spacing (160 m) was too coarse to resolve buildings. Air flows around buildings were successfully simulated in Domain 3 and air flows modified in Domain 3 were transferred back to Domain 2 and Domain 1 through two-way nesting algorithm.

A few atmospheric models have both mesoscale and CFD scale modeling capabilities. However, we are not aware of any report that a single model was used to simulate interactions between mesoscale and CFD scale circulations.

REFERENCES

Brown, M.J., Lawson, R.E., DeCroix, D., and Lee R.L., 2001: Comparison of Centerline Velocity Measurements Obtained Around 2D and 3D Building Arrays in a Wind Tunnel. *Proceedings of the 2001 Internatinal Symposium on Environmental Hydraulic, Tempe, AZ, December 2001.*

Hirt, C.W., and J. L. Cox, 1972: Calculating Three-Dimensional Flows around Structures and over Rough Terrain. *J. of Computational Phys*., **10**, 324-340.

Kao, C.-Y. J. and Yamada, T., 1988: Use of the CAPTEX Data for Evaluation of a Long-Range Transport Numerical Model with a Four-Dimensional Data Assimilation Technique, *Monthly Weather Review*, **116**, pp. 293-206.

Mellor, G. L., and T. Yamada, 1974: A Hierarchy of Turbulence Closure Models for Planetary Boundary Layers. *J. of Atmos. Sci*., **31**, 1791-1806.

Mellor, G. L., and T. Yamada, 1982: Development of a Turbulence Closure Model for Geophysical Fluid Problems. *Rev. Geophys. Space Phys*., **20**, 851-875.

United Nations, World Urbanization Prospects, The 1999 revision.

United Nations, World Urbanization Prospects, The 2003 revision.

Yamada, T., 1983: Simulations of Nocturnal Drainage Flows by a q^2l Turbulence Closure Model. *J. of Atmos. Sci*., **40**, 91-106.

Yamada, T., and S. Bunker, 1988: Development of a Nested Grid, Second Moment Turbulence Closure Model and Application to the 1982 ASCOT Brush Creek Data Simulation. *Journal of Applied Meteorology*, **27**, 562-578.